https://doi.org/10.1016/j.orgel.2020.105732

Achieving efficient green-solvent-processed organic solar cells by employing *ortho-ortho* perylene diimide dimer

Helin Wang [a,b,c], Jiatao Wu [a], Youming Zhang [a], Jun Song [a, *], Lingcheng Chen [c], Yi Xiao [c, *], Junle Qu [a], Wai-Yeung Wong [b, *]

[a] Key Laboratory of Optoelectronic Devices and Systems of Ministry of Education and Guangdong Province, College of Physics and Optoelectronic Engineering, Shenzhen University, Shenzhen 518060, P. R. China.

[b] Department of Applied Biology and Chemical Technology, The Hong Kong Polytechnic University, Hung Hom, Hong Kong, P. R. China.

[c] State Key Laboratory of Fine Chemicals, Dalian University of Technology, Dalian, 116024, P. R. China.

[*] Corresponding author.

Email addresses: songjun@szu.edu.cn (J. Song); xiaoyi@dlut.edu.cn (Y. Xiao); wai-yeung.wong@polyu.edu.hk (W.-Y. Wong)

The Supporting Information includes materials and characterization, device fabrication and measurement, synthesis of compound oo-2PDI, and supporting tables and figures.

Abstract: The lack of electron acceptors with suitable green solvent processing and excellent device performance is an important problem that hinders the development and commercialization of organic solar cells (OSCs). Here, an *ortho-ortho* perylene diimide (PDI) dimer (*oo*-2PDI) is developed and used as an acceptor for use in efficient green-solvent-processed (GSP) OSCs. By using chlorobenzene (CB), anisole, and *o*-xylene as the processing solvents, power conversion efficiencies (*PCE*s) of 5.04%, 5.03%, and 5.78% were achieved without the additive, respectively. In addition, the non-fullerene *oo*-2PDI-based GSPOSCs show superior photovoltaic performance to [6,6]-phenyl-C_{61}-butyric acid methyl ester (PCBM)-based GSPOSCs under identical

conditions. Therefore, these results demonstrate the possibility of achieving efficient non-fullerene GSPOSCs.

Keywords: *perylene diimide; electron acceptor; ortho-ortho dimer; green solvent; organic solar cell.*

1. Introduction

Bulk heterojunction (BHJ) OSCs represent a novel approach of utilizing solar energy because of their low cost, lightweight, solution-processability, and ease of chemical modification [1-3]. To obtain a higher *PCE*, it is necessary to ensure excellent phase separation of the donor and acceptor via solution-processing. To date, halogenated solvents, such as chlorobenzene (CB) or *o*-dichlorobenzene (DCB) have typically been used to obtain high-efficiency BHJOSCs, but the toxicity of such halogenated solvents has become a huge obstacle to the commercialization of OSCs [4-10]. To overcome this, low-toxicity and environmentally-friendly non-halogenated solvents are better choices for OSCs [11-13]. Consequently, material design and solvent selection are two important factors to achieving high-performance green-solvent-processed (GSP) OSCs [14-16]. In order to improve the solubility of materials in green solvents, side-chain engineering is an outstanding method for small molecules or polymers without changing the material's other intrinsic properties [17-19]. For instance, to increase the solubility in the 2-methyltetrahydrofuran, two novel polymers with ethylenedioxythiophene side chains were developed to fabricate the ternary blend GSPOSCs [20]. As a result, the devices increased the best PCE to 12.26% with a high fill factor of 75.6%. In addition, Li et al. [21] applied fluorine and alkylsilyl substitutions in the polymer framework to reduce the energy levels and increase the absorption coefficient. The GSPOSCs achieved a high PCE of 12.8% owing to the excellent modification of the chemical structure. However, compared with a number of modified electron donors, the research on proper electron

acceptors is lagging behind, which restricts the development of high-performance GSPOSCs [22, 23]. Therefore, the design and synthesis of electron acceptors with excellent solubility and photovoltaic performance is a key challenge for GSPOSCs.

Furthermore, the green solvents meet some requirements: enough solubility for organic semiconductor, suitable boiling point, and saturation vapor pressure. As far as we know, Anisole and *o*-xylene are two excellent non-halogenated solvent candidates for use in developing efficient GSPOSCs [24]. However, many electron acceptors have poor solubility in anisole and *o*-xylene, which results in unfavorable morphologies that limit the improvements in the device performance [25-27]. Fullerene derivatives are commonly used as electron acceptors in OSCs, but they have several disadvantages that have limited their use in GSPOSCs, including their weak absorption in the visible region, high cost, and difficulty in modifying their chemical structures [28-30]. Currently, a lot of attention has been drawn to perylene diimide (PDI) dimers as excellent electron acceptors in non-fullerene OSCs because of their lower cost, ease of functionalization, strong absorption, suitable energy levels, and high electron transport properties [31, 32]. In addition, the solubility of PDI dimers in environmentally-friendly solvents can be easily improved by modifying the side chains of PDI units, which can help obtain suitable electron acceptors for GSPOSCs. Among the PDI dimers, our previous work explored an *ortho-ortho* PDI dimer (*oo*-2PDI) to fabricate non-fullerene OSCs with the *PCE*s greater than 8%, which indicates that *ortho-ortho* PDI dimers have great potential as highly-efficient electron acceptors for GSPOSCs [33]. Importantly, the use of *ortho-ortho* PDI derivatives to achieve efficient GSPOSCs has rarely been reported. Thus, it is of great interest to obtain a *PCE* breakthrough for non-fullerene *ortho-ortho* PDI dimer-based GSPOSCs.

Herein, a systematic investigation has been performed on the influence of three solvents (CB, anisole, and *o*-xylene) on the performance of poly[[4,8-bis[5-(2-ethylhexyl)-2-thienyl]benzo[1,2-b:4,5-b']dithiophene-2,6-diyl][2-(2-ethyl-1-oxohexyl)thieno[3,4-b]t

hiophenediyl]] (PBDTTT-C):*oo*-2PDI-based devices, and the structures of PBDTTT-C and *oo*-2PDI are shown in Figure 1a. By using *o*-xylene as the processing solvent, the *PCE* was improved to 5.78%, which is higher than that of the devices using CB (5.04%) or anisole (5.03%). In addition, the *oo*-2PDI-based devices exhibited better photovoltaic performance than the PCBM-based devices under identical conditions, which can be attributed to the favorable morphology, decreased charge recombination, and balanced charge transport. These results reveal that *ortho-ortho* PDI dimers have promising potential to successfully replace PCBM to develop efficient GSPOSCs.

2. Results and discussion

2.1 Optical and electrochemical properties

PBDTTT-C and PCBM were purchased from Derthon Optoelectronic Materials Co., and *oo*-2PDI was synthesized using a previously-reported method [33]. *oo*-2PDI exhibits excellent solubility in CB (over 30 mg/mL), anisole (over 20 mg/mL), and *o*-xylene (over 20 mg/mL) because of its linear conjugated framework and herringbone side chains. The thin-film UV-Vis absorption spectra of *oo*-2PDI and PCBM are presented in Figure 1b. In the thin films, *oo*-2PDI shows strong absorption from 400 to 600 nm, while PCBM shows strong absorption in the near-ultraviolet region and weak absorption in the visible region. Consequently, *oo*-2PDI has better visible absorption than PCBM, which can help generate photocurrent and improve the device performance. The absorption spectra of *oo*-2PDI displays a slight redshift of about 6 nm compared with that in dichloromethane solution, as shown in Figure S1. These results imply that the distortion of the conjugated framework of *oo*-2PDI prevents intermolecular aggregation, which helps achieve favorable morphologies in the blend films. Furthermore, polymer PBDTTT-C exhibits a strong absorption from 500 to 800 nm, which is complementary to *oo*-2PDI and PCBM, respectively, and will thus help with light harvesting to improve the device performance.

To investigate the electrochemical properties of PCBM and *oo*-2PDI, cyclic

voltammetry (CV) was carried out and the results are depicted in Figure 1c. The LUMO level of *oo*-2PDI was estimated to be -3.9 eV, which is close to that of PCBM (-3.8 eV). In addition, *oo*-2PDI showed outstanding solubility in common organic solvents because of its herringbone side chain and nonplanar conjugated framework. These results show that *oo*-2PDI has excellent solubility and suitable LUMO levels and can be used as an acceptor in GSPOSCs.

2.2 Performance of organic solar cells

The photovoltaic performance of non-fullerene OSCs fabricated from PBDTTT-C:*oo*-2PDI was systematically characterized using different processing solvents. Figure 2a shows that the inverted OSCs were fabricated with a device structure of ITO/ZnO/active layer/MoO_3/Al due to ease of manufacturing and proven environmental stability, as well as the energy level alignments of the OSCs shown in Figure 2d. Since the primary goal of this research is to study the influence of three solvents (CB, anisole, and *o*-xylene) on the photovoltaic performance of non-fullerene OSCs, the active layers were deposited by spin-coating them from three different solutions with varying D/A ratios. The *J-V* curves are presented in Figure 2b and Figures S2-S5, and the results are summarized in Table 1 and Tables S1 for a clearer comparison. The optimal blended ratio was found to be 1:1 for all three solvents without the additive. In addition, the *o*-xylene-based device shows the best performance, with a V_{oc} of 0.77 V, a J_{sc} of 16.2 mA cm^{-2}, an *FF* of 0.46, and a *PCE* of 5.78%. In contrast, the two CB- and anisole-based devices show inferior *PCE* values of 5.04% and 5.03%, respectively. In particular, a lower J_{sc} can be attributed to the unfavorable morphologies and unbalanced charge transport.

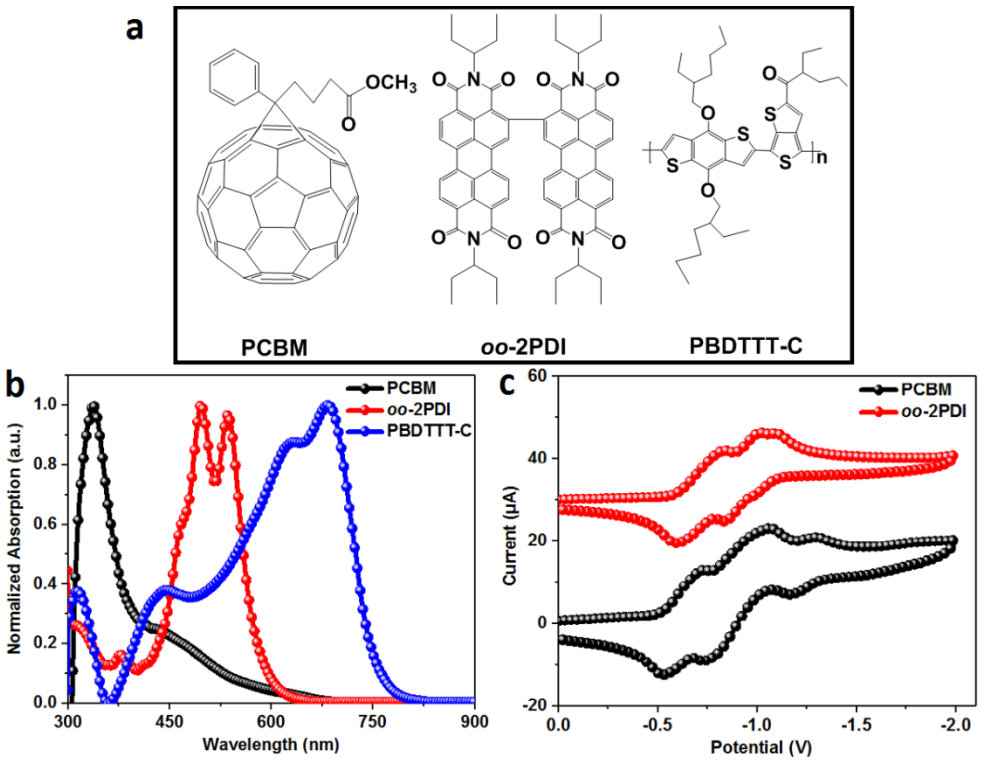

Figure 1. (a) The structures of an electron acceptor *oo*-2PDI and one polymer donor PBDTTT-C; (b) UV-Vis absorption spectra of donor and two acceptors obtained in films; (c) cyclic voltammetry of PCBM and *oo*-2PDI obtained in solution.

Table 1. Device parameters of the OSCs based on PCBM and *oo*-2PDI using different solvents.

Active layers	Solvents	D/A ratio [wt/wt]	J_{sc} [mA cm^{-2}]	V_{oc} [V]	*FF* [%]	*PCE* [%]
PBDTTT-C:*oo*-2PDI	chlorobenzene	1:1	14.5	0.76	45.9	5.04
PBDTTT-C:*oo*-2PDI	anisole	1:1	13.7	0.78	47.0	5.03
PBDTTT-C:*oo*-2PDI	*o*-xylene	1:1	16.2	0.77	45.9	5.78
PBDTTT-C: PCBM	*o*-xylene	1:1	13.8	0.76	45.6	4.77

To gain further insight into the differences in the photovoltaic performance of the two acceptors (*oo*-2PDI and PCBM), PBDTTT-C:PCBM-based devices were fabricated, and the blend films were processed under the same conditions as before. As a result, the PCBM-based OSC using *o*-xylene reached a relatively low *PCE* of 4.77% with a V_{oc} of 0.76 V, a J_{sc} of 13.8 mA cm^{-2}, and an *FF* of 0.46. These results reveal that the *ortho-ortho*

PDI dimer has promising potential as an efficient electron acceptor and can achieve higher *PCE* values than PCBM in GSPOSCs.

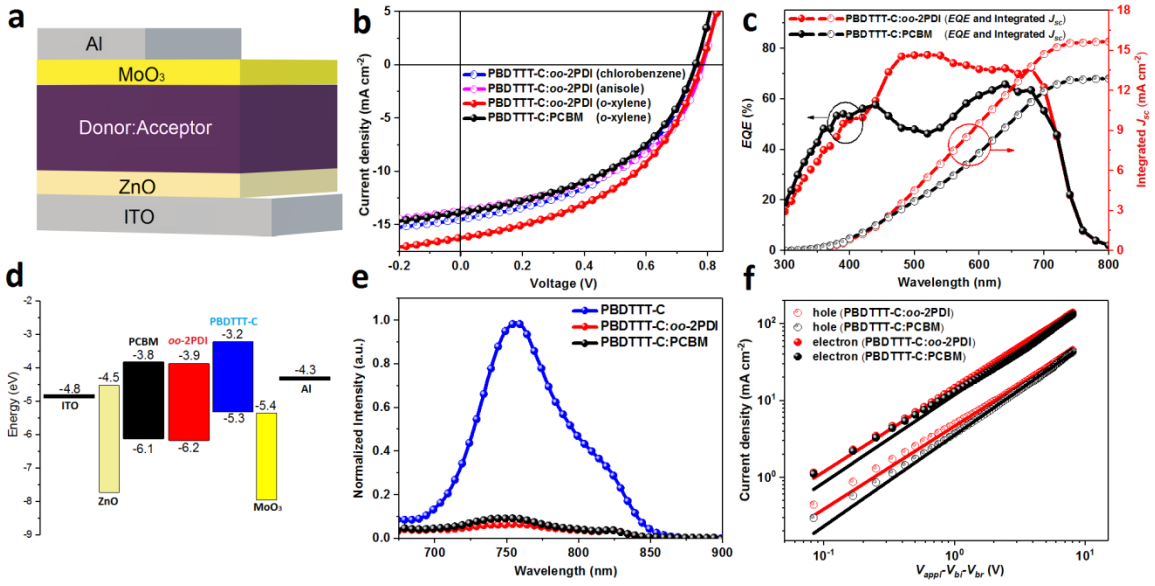

Figure 2. (a) Device structure of the OSCs fabricated in this work; (b) *J-V* curves of OSCs based on *oo*-2PDI and PCBM as acceptors with the different processing solvents; (c) *EQE* curves and the integrated J_{sc} for the *oo*-2PDI- and PCBM-based devices; (d) energy level alignments of OSCs; (e) steady-state photoluminescence spectra of pure donor and two blend films; (f) current density-voltage traces of different charge transport devices based on *oo*-2PDI and PCBM by the SCLC method.

The *EQE* curves of two GSPOSCs are displayed in Figure 2c. The photoresponse spectra of the two devices based on PCBM and *oo*-2PDI cover the 300 to 800 nm range, which is attributed to the contribution of the donor and acceptor, which closely agrees with their thin-film absorptions. Figure 2c shows that the device based on PBDTTT-C:*oo*-2PDI showed a strong photoresponse with a maximum value of 78% at 520 nm, demonstrating efficient photon harvesting and excellent charge collection. In contrast, the PCBM-based device exhibited a lower photoresponse from 300 to 600 nm, mainly because of the weak absorption of PCBM in the visible region. Meanwhile, due to

the improved photoresponse of the *oo*-2PDI-based device, an integrated J_{sc} of 15.7 mA cm^{-2} was obtained, which is higher than that of the PCBM-based device (13.0 mA cm^{-2}). This shows that the *J-V* measurement results are accurate within a 5% error.

2.3 Photoluminescence quenching and charge transport properties

To examine the exciton dissociation efficiency at the donor/acceptor interface, photoluminescence (PL) spectra of the pure donor film and two blended films were obtained. Figure 2e shows that the pure donor film exhibits a strong fluorescent emission, while two blended films display obvious PL quenching with the quenching efficiencies of 87.6% and 90.0%, respectively. As shown in Figure S6, the exciton lifetimes of two blend films are apparently reduced compared with that of pure donor film, which is consistent with the PL measurement results. These results suggest that efficient photoinduced charge separation occurred between the donor and acceptor, where PBDTTT-C/*oo*-2PDI showed a stronger quenching efficiency than PBDTTT-C/PCBM. In addition, utilizing the space charge limited current (SCLC) method, both the hole (μ_h) and electron (μ_e) mobilities based on the two blend films were measured [20]. Measurements were conducted using the devices with structures of ITO/PEDOT:PSS/Active layer/MoO_3/Al (hole-only) and ITO/ZnO/Active layer/Ca/Al (electron-only). Figure 2f shows the traces of the current density-actual voltage extracted from the experimental data, and the relevant data are summarized in Table S2. Both μ_h and μ_e of the *oo*-2PDI-based device are higher than those of PCBM under identical conditions. This indicates that high charge carrier mobility data can explain the high charge injection and transport observed in the *oo*-2PDI-based OSCs to efficiently improve the device performance. Moreover, the ratios of hole/electron mobilities (μ_h/μ_e) were 6.5 and 7.0 for PBDTTT-C:*oo*-2PDI and PCBM blend films, respectively, implying that more balanced charge transport is present in the *oo*-2PDI-based device than that of PCBM. Therefore, high and balanced charge transport can give superior performance in *oo*-2PDI-based OSCs, but PCBM was not used.

2.4 Film morphology

The surface morphologies of PBDTTT-C:*oo*-2PDI and PCBM blend films processed under identical conditions were observed by atomic force microscopy (AFM). Figure 3a, 3b, 3d and 3e show that the surface of the oo-2PDI and PCBM blend films have different root mean square (RMS) roughness values of 0.63 nm and 1.01 nm, respectively. This indicates that the smooth and uniform morphology of PBDTTT-C:*oo*-2PDI helps obtain continuous pathways to achieve efficient charge separation and transport. Meanwhile, the PCBM-based film showed more aggregation domains compared with the *oo*-2PDI-based film, as determined from their height images. Moreover, the increase in the roughness of PCBM-based films indicates that large grains were formed due to the use of *o*-xylene as the processing solvent, which is also responsible for its decreased J_{sc} and *PCE* values.

2.5 Charge carrier recombination

Light-intensity-dependent characteristics were used to evaluate the exciton dissociation and charge recombination processes of the two GSPOSCs [34, 35]. Exciton dissociation rates (P_c), as well as the photo-generated current density (J_{ph}) versus the effective voltage (V_{eff}), traces of the two devices were obtained and are displayed in Figure 3c. P_c values of 88% and 90% for PCBM- and *oo*-2PDI-based devices were obtained, respectively. This indicates that more efficient exciton dissociation occurs in *oo*-2PDI-based devices compared with PCBM, which can be attributed to the favorable morphology and balanced charge transport present in the former. The light intensity (P) dependence of J_{sc} was measured to examine how charge recombination in the two blend films affected the device performance using the relationship $J_{SC} \propto P^S$. The values of the scaling factor (S) fitted and calculated from the J_{sc}-P traces are 0.85 and 0.90 for PCBM and *oo*-2PDI, respectively, as shown in Figure 3f. As a result, *oo*-2PDI-based devices exhibit efficient exciton dissociation and decreased charge recombination compared with

PCBM-based devices, which help enhance the efficiency of the GSPOSCs.

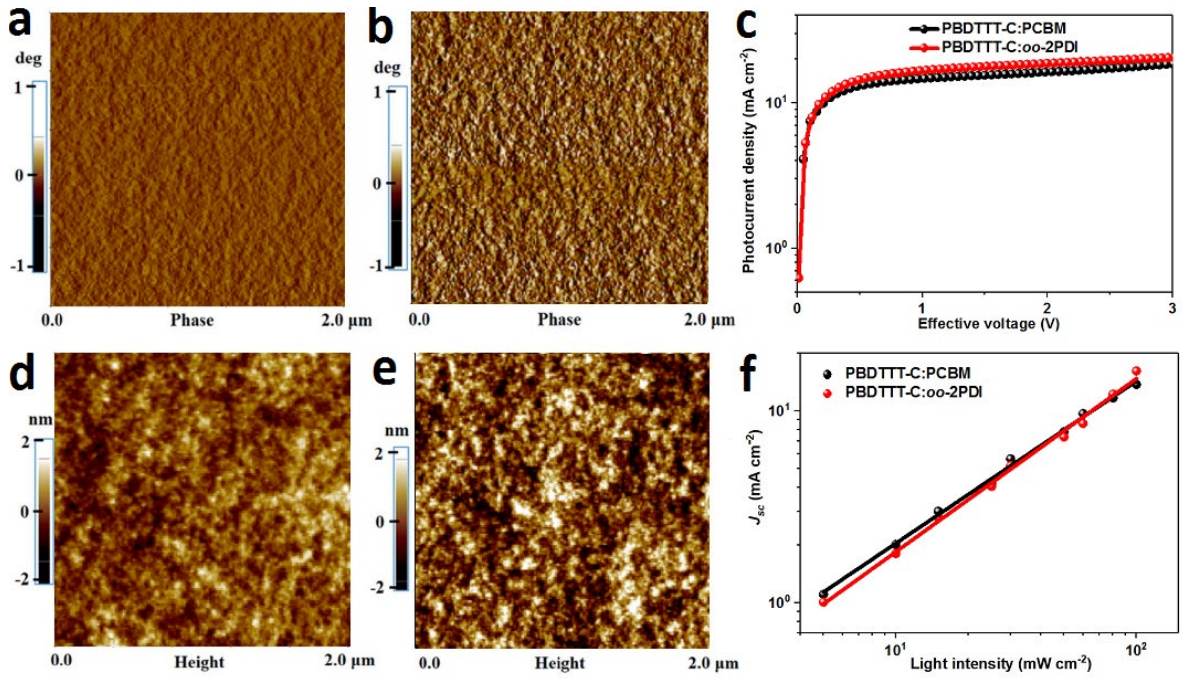

Figure 3. AFM images of the blend films based on *oo*-2PDI (a, b) and PCBM (d, e); photocurrent density-effective voltage traces (c) and short circuit current density-light intensity traces (f) of the devices based on *oo*-2PDI and PCBM.

3. Conclusion

A simple structure of *ortho-ortho* perylene diimide (PDI) dimer, namely *oo*-2PDI, was developed and used as an efficient electron acceptor for the OSCs. PBDTTT-C:*oo*-2PDI-based devices were fabricated to investigate the effects of different solvents on the device performance. As a result, *PCE* values of 5.04%, 5.03%, and 5.78% were achieved using CB, anisole, and *o*-xylene without the additive, respectively. Interestingly, it was found that the *o*-xylene-based GSPOSC exhibited a higher *PCE* than the devices using CB and anisole, indicating that *oo*-2PDI has a great potential as an efficient acceptor for the GSPOSCs. Due to its favorable morphology, improved exciton dissociation, decreased charge recombination, and balanced charge transport, the

oo-2PDI-based GSPOSCs obtained using *o*-xylene showed better performance than the PCBM-based devices under identical conditions. Therefore, these results open new paths for obtaining efficient non-fullerene GSPOSCs and the promise for the commercialization of OSCs.

Acknowledgment

This work has been partially supported by the National Key R&D Program of China (2018YFC0910602); the National Natural Science Foundation of China (61775145, 61525503, 61620106016, 61835009, 81727804, 61804099); the China Postdoctoral Science Foundation Funded Project (2018M643147, 2019T120747); (Key) Project of Department of Education of Guangdong Province (2015KGJHZ002, 2016KCXTD007); and Shenzhen Basic Research Project (JCYJ20170412110212234, JCYJ20170412105003520). W.-Y. Wong would like to thank the Hong Kong Research Grants Council (PolyU 123384/16P), Hong Kong Polytechnic University (1-ZE1C, C5037-18G) and Ms. Clarea Au (847S) for the financial support.

References

[1] Zhao J, Li Y, Yang G, Jiang K, Lin H, Ade H, Ma W, Yan H, Efficient organic solar cells processed from hydrocarbon solvents, Nat. Energy 1 (2014) 15027-15033.

[2] Lu L, Zheng T, Wu Q, Schneider AM, Zhao D, Yu L, Recent advances in bulk heterojunction polymer solar cells, Chem. Rev. 115 (2015) 12666-12731.

[3] Lin Y, Wang J, Zhang ZG, Bai H, Li Y, Zhu D, Zhan X, An electron acceptor challenging fullerenes for efficient polymer solar cells, Adv. Mater. 27 (2015) 1170-1174.

[4] Yuan J, Ma W, High efficiency all-polymer solar cells realized by the synergistic effect between the polymer side chain structure and solvent additive, J. Mater. Chem. A 3 (2015) 7077-7085.

[5] Hartnett PE, Timalsina A, Matte HSSR, Zhou N, Guo X, Zhao W, Facchetti AR, Chang PH, Hersam MC, Wasielewski MR, Marks TJ, Slip-Stacked perylenediimides as an alternative strategy for hign efficiency nonfullerene acceptors in organic photovoltaics, J. Am. Chem. Soc. 136 (2015) 16345-16356.

[6] Dayneko SV, Hendsbee AD, Welch GC, Fullerene-free polymer solar cells processed from non-halogenated solvents in air with PCE of 4.8%, Chem. Commun. 53 (2017) 1164-1167.

[7] Hwang YJ, Earmme T, Courtright BAE, Eberle FN, Jenekhe SA, N-Type semiconducting naphthalene diimide-perylene diimide copolymers: controlling crystallinity, blend morphology, and compatibility toward high-performance all-polymer solar cells, J. Am. Chem. Soc. 137 (2015) 4424-4434.

[8] Zhao D, Wu Q, Cai Z, Zheng T, Chen W, Lu J, Yu L, Electron acceptors based on α-substituted perylene diimide (PDI) for organic solar cells, Chem. Mater. 28 (2016) 1139-1146.

[9] Wang H, Chen L, Xiao Y, Constructing a donor-acceptor linear conjugation structure for heterologous perylene diimides to greatly improve the photovoltaic performance, J. Mater. Chem. C 7 (2019) 835-842.

[10] Zhong Y, Trinh MT, Chen R, Purdum GE, Khlyabich PP, Sezen M, Oh S, Zhu H, Fowler B, Zhang B, Wang W, Nam CY, Sfeir MY, Black CT, Steigerwald ML, Loo YL, Ng F, Zhu XY, Nuckolls C, Molecular helices as electron acceptors in high-performance bulk heterojunction solar cells, Nat. Commun. 6 (2015) 8242-8250.

[11] Xu X, Yu T, Bi Z, Ma W, Li Y, Peng Q, Realizing Over 13% Efficiency in Green-Solvent-Processed Nonfullerene Organic Solar Cells Enabled by 1,3,4-Thiadiazole-Based Wide-Bandgap Copolymers, Adv. Mater. 30 (2018) 1703973.

[12] Chen Y, Cui Y, Zhang S, Hou J, Molecular design toward efficient polymer solar cells processed by green solvents, Polym. Chem. 6 (2015) 4089-4095.

[13] Henson Z, Zalar P, Chen X, Welch G, Nguyen T, Bazan G, Towards environmentally friendly processing of molecular semiconductors, J. Mater. Chem. A 1 (2013) 11117-11120.

[14] Pramanik C, Li Y, Singh A, Lin W, Hodgson J, Briggs J, Ellis S, Müller P, McGruer N, Miller G, Water soluble pentacene, J. Mater. Chem. C 1 (2013) 2193-2201.

[15] Chen X, Liu X, Burgers M, Huang Y, Bazan G, Green-Solvent-Processed Molecular Solar Cells, Angew Chem. Int. Ed. 53 (2014) 14378.

[16] Meng B, Song H, Chen X, Xie Z, Liu J, Wang L, Replacing alkyl with oligo(ethylene glycol) as side chains of conjugated polymers for close π-π stacking, Macromolecules 48 (2015) 4357-4363.

[17] Wei H, Jin G, Wang L, Hao L, Na T, Wang Y, Tian W, Sun H, Zhang H, Wang H, Zhang H, Yang B, Synthesis of a water-soluble conjugated polymer based on thiophene for an aqueous-processed hybrid photovoltaic and photodetector device, Adv. Mater. 26 (2014) 3655-3662.

[18] Yao X, Shao W, Xiang X, Xiao W, Liang L, Zhao F, Ling J, Lu Z, Li J, Li W, Side chain engineering on a small molecular semiconductor: Balance between solubility and performance by choosing proper positions for alkyl side chains, Org. Electron. 61 (2018) 56-64.

[19] Li Z, Ying L, Zhu P, Zhong W, Li N, Liu F, Huang F, Cao Y, A generic green solvent concept boosting the power conversion efficiency of all-polymer solar cells to 11%, Energy Environ. Sci. 12 (2019) 157-163.

[20] Liao C, Zhang M, Xu X, Liu F, Li Y, Peng Q, Green solvent-processed efficient non-fullerene organic solar cells enabled by low-bandgap copolymer donors with EDOT side chains, J. Mater. Chem. A 7 (2019) 716-726.

[21] Su W, Li G, Fan Q, Zhu Q, Guo X, Chen J, Wu J, Ma W, Zhang M, Li Y, Nonhalogen solvent-processed polymer solar cells based on chlorine and trialkylsilyl

substituted conjugated polymers achieve 12.8% efficiency, J. Mater. Chem. A 7 (2019) 2351-2359.

[22] Welsh T, Laventure A, Alahmadi A, Zhang G, Baumgartner T, Zou Y, Jäkle F, Welch G, Borane incorporation in a non-fullerene acceptor to tune steric and electronic properties and improve organic solar cell performance, ACS Appl. Energy Mater. 2 (2019) 1229-1240.

[23] Zhao W, Zhang S, Zhang Y, Li S, Liu X, He C, Zheng Z, Hou J, Environmentally friendly solvent-processed organic solar cells that are highly efficient and adaptable for the blade-coating method, Adv. Mater. (2017) 1704837.

[24] Zhang S, Ye L, Zhang H, Hou J, Green-solvent-processable organic solar cells, Mater. Today 16 (2016) 533-543.

[25] Lin Y, Zhan X, Oligomer molecules for efficient organic photovoltaics, Acc. Chem. Res. 49 (2016) 175-183.

[26] An Q, Zhang F, Zhang J, Tang W, Deng Z, Hu B, Versatile ternary organic solar cells: a critical review, Energy Environ. Sci. 9 (2016) 281-322.

[27] Kobaisi MA, Bhosale SV, Latham K, Raynor AM, Bhosale SV, Functional naphthalene diimides: synthesis, properties, and applications, Chem. Rev. 116 (2016) 11685-11796.

[28] Yan C, Barlow S, Wang Z, Yan H, Jen AKY, Marder SR, Zhan X, Non-fullerene acceptors for organic solar cells, Nat. Rev. Mater. 3 (2018) 18003.

[29] Cheng P, Li G, Zhan X, Yang Y, Next-generation organic photovoltaics based on non-fullerene acceptors, Nat. Photonics 12 (2018) 131-142.

[30] Chen W, Zhang Q, Recent progress in non-fullerene small molecule acceptors in organic solar cells (OSCs), J. Mater. Chem. C 5 (2017) 1275-1302.

[31] Liu J, Chen S, Qian D, Gautam B, Yang G, Zhao J, Bergqvist J, Zhang F, Ma W, Ade H, Inganäs O, Gundogdu K, Gao, F, Yan H, Fast charge separation in a non-fullerene organic solar cell with a small driving force, Nat. Energy 1 (2016) 16089-16095.

[32] Meng D, Fu H, Xiao C, Meng X, Winands T, Ma W, Wei W, Fan B, Huo L, Doltsinis NL, Li Y, Sun Y, Wang Z, Three-bladed rylene propellers with three-dimensional network assembly for organic electronics, J. Am. Chem. Soc. 138 (2016) 10184-10190.

[33] Wang H, Chen L, Xiao Y, A simple molecular structure of ortho-derived perylene diimide diploid for non-fullerene organic solar cells with efficiency over 8%, J. Mater. Chem. A 5 (2017) 22288-22296.

[34] Zhang Y, Guo X, Guo B, Su W, Zhang M, Li Y, Nonfullerene polymer solar cells based on a perylene monoimide acceptor with a high open-circuit voltage of 1.3 V, Adv. Funct. Mater. 27 (2017) 1603892.

[35] Li S, Zhang H, Zhao W, Ye L, Yao H, Yang B, Zhang S, Hou J, Green-solvent-processed all-polymer solar cells containing a perylene diimide-based acceptor with an efficiency over 6.5%, Adv. Energy Mater. (2015) 1501991.